Excited State Dynamics and Heterogeneity of Folded and Unfolded States of Cytochrome *c*

Ralph Jimenez and Floyd E. Romesberg*

Department of Chemistry, The Scripps Research Institute, 10550 N. Torrey Pines Road, Maildrop CVN22, La Jolla, California 92037

Received: April 11, 2002; In Final Form: June 10, 2002

Cytochrome *c* is an electron transfer protein whose redox and folding properties have received a great deal of attention. In this study, transient absorption, transient grating, and three pulse photon echo peak shift (3PEPS) measurements have been used to characterize the photophysics of the heme chromophore in the folded protein and in two different unfolded proteins. The data are interpreted in terms of a reactive three level system. A Soret excited state lifetime of 40 to 50 fs is observed, which is not sensitive to the folded state of cytochrome *c*. An intermediate time scale of 200 to 400 fs is also observed, which may be associated with the Q state lifetime. The longest time scale, assigned to ground state recovery, is approximately 2 to 4 ps. The dynamics are discussed in terms of the folded and redox states of the protein. The 3PEPS data show that the folded protein has little structural heterogeneity; however, the unfolded proteins show a larger degree of structural heterogeneity, the extent of which depends on the unfolding conditions.

I. Introduction

Cytochrome *c* (cyt *c*), a small heme protein that functions as an electron carrier in the respiratory chain, has been one of the most intensively studied redox proteins.[1] The protein is composed of a single polypeptide chain with a heme cofactor covalently attached through thioether linkages with two cysteine residues. The Fe atom of the heme, which may exist in either the oxidized Fe(III) or reduced Fe(II) state, is also ligated by two protein side chains, His18 and Met80. Crystal structures of cyt *c* show a largely α-helical protein with a buried heme cofactor. The heme is tightly packed by hydrophobic side chains and distorted from planarity to a propeller-like geometry.[2] Cyt *c* has also been used extensively to study protein folding,[3] exhibiting reversible unfolding under a variety of conditions, including high temperature,[4] extreme pH or ionic strength,[5,1] and high concentrations of small molecule denaturants such as urea.[6,7] Because the heme is covalently attached to the peptide, the chromophore remains intimately associated with the protein under all conditions. This forced association between the heme and the protein makes the chromophore a sensitive spectroscopic probe of the protein environment, both in the folded and unfolded states.

The steady state absorption spectra of cyt *c* are well known.[8] The most intense transition ($\epsilon \sim 10^5$ M^{-1} cm^{-1}) gives rise to the Soret (or B) band, which occurs at 409 nm for the oxidized protein and 416 nm for the reduced form. The next most intense absorption ($\epsilon \sim 10^4$ M^{-1} cm^{-1}) is the Q band, which shows two peaks (520 and 550 nm) for the reduced protein but only one broad absorption for the oxidized protein. The electronic transitions that give rise to the B and Q bands involve predominantly porphyrin orbitals ($\pi-\pi^*$) with a small component of metal orbitals. The spectrum of cyt *c* also shows a weaker absorption ($\epsilon \sim 10^3$ M^{-1} cm^{-1}) at 695 nm, present in both oxidation states, that results from charge transfer from the Fe to the Met80 ligand. In addition to the redox state dependence, these bands are known to reflect the conformation of the protein (Figure 1).[4−7] The 409 nm Soret absorption band in the oxidized protein has a width (full width half-maximum, fwhm) of 1600 cm^{-1}. At pH 2.0, the absorption maximum shifts to 395 nm, with a fwhm of 1908 cm^{-1}. The blue-shift of the Soret band upon unfolding the protein is thought to result from a more polar environment as well as a ligand substitution at the iron center.[5] In 9 M urea (pH 2.0), the Soret band also peaks at 395 nm, but narrows to 1388 cm^{-1}.

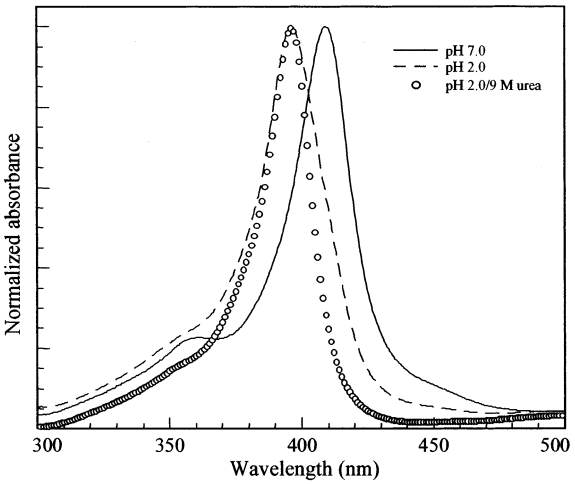

Figure 1. UV−vis absorption spectra of oxidized cyt *c* in pH 7, pH 2, and urea (pH 2) solutions.

The emission spectra of cyt *c* have been less useful than the absorption spectra, because little fluorescence is detectable in either redox state of the protein. The reduced protein does not show Soret band emission, but does show a very low yield of Q band emission when excited in the B band ($\phi_F = 5 \times 10^{-7}$) or Q band ($\phi_F = 4 \times 10^{-6}$).[9,10] In contrast, the oxidized protein does not show Q band fluorescence. These extremely low fluorescence yields imply that there is ultrafast relaxation of both the B and Q states, which implies that both absorption bands may be significantly lifetime broadened. This homogeneous broadening complicates the spectroscopic study of cyt *c*.[11−14]

10.1021/jp0209648 CCC: $22.00
Published on Web 08/03/2002

Interpretation of the cyt *c* spectra is further complicated by variable and unknown quantities of inhomogeneous broadening. For example, changes in the fwhm of the Soret band upon denaturation may reflect different amounts of inhomogeneous broadening. However, resonance Raman studies show that as cyt c unfolds the heme geometry becomes more planar, which causes a decrease in the intensity of low-frequency out-of-plane vibrational modes.[15] Thus, the homogeneous line width may not be constant, and therefore it cannot be assumed that the observed changes in the width of the Soret band arise from inhomogeneous effects, alone. This complex behavior mandates a careful dissection of inhomogeneous and homogeneous contributions to the Soret bandwidth.

Femtosecond time-resolved spectroscopic measurements are a powerful means of deconvoluting a spectrum into its homogeneous and inhomogeneous components. For example, transient absorption (TA) and transient grating (TG) measurements can be used to reveal time scales of solvent and population dynamics, whereas echo spectroscopies such as the three pulse echo peak shift (3PEPS) are sensitive to the amplitude and time scales of environmental fluctuations.[16] These techniques have been used to study solvation dynamics in liquids,[16−21] glasses,[22,23] and proteins.[24−28] Recently, the flexibility of an antibody binding site has also been characterized.[29] The 3PEPS experiment is also sensitive to the presence of inhomogeneous broadening and has been used, for example, to characterize the diversity of solute environments in a glass.[22] In most of these studies the chromophore has a long-lived excited state. Chromophores with short-lived excited states, such as hemes, have proven more difficult to study. Recently, Fleming and co-workers have developed an approach for incorporating the effects of ultrafast internal conversion.[30−32] Similar approaches permit the characterization of hemoproteins such as cyt *c*.

In this study, the dynamics of folded, acid-unfolded, and urea (pH 2.0) unfolded states of cyt *c* are measured using femtosecond nonlinear spectroscopy of the Soret band. The measurements contain information on the lifetimes and dynamics of the B and Q states. A kinetic model for the nonlinear signal is derived that includes the effects of internal conversion from the B and Q states in both the folded and unfolded proteins. The relative contributions of protein conformational diversity and cofactor vibrations to the Soret band line shape are discussed. Significant inhomogeneous broadening is found to be present in the spectra of the unfolded proteins but not in the spectrum of the folded protein. A connection between inhomogeneous broadening and conformational diversity of the unfolded protein is proposed.

II. Experimental Section

A description of the ultrafast laser system and optical arrangement used for these measurements has been published previously.[29] Laser wavelengths of 400 nm for the unfolded proteins and 407 nm for the folded protein were used. The pulse durations were 35 to 40 fs (fwhm). Horse-heart cyt *c* was purchased from Sigma, and quantitatively oxidized with a 10-fold molar excess of bis(dipicolinate) cobaltate(III). The oxidant was removed by gel filtration with Sephadex G-15 (AP Biotech). Aliquots of the oxidized protein were then lyophilized and frozen. Immediately prior to experiment, samples were thawed and dissolved in one of three solutions: 100 mM sodium phosphate buffer, pH 7.0 (referred to as pH 7 or folded), 100 mM sodium phosphate with pH adjusted to 2.0 by adding HCl (referred to as pH 2.0 unfolded), or 100 mM sodium phosphate, pH 2.0, with 9 M urea (referred to as urea (pH 2.0) unfolded).

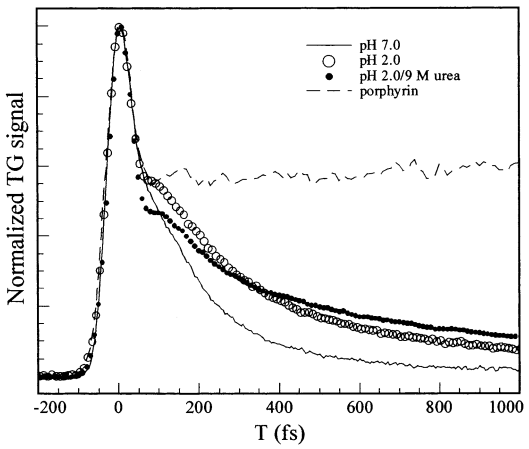

Figure 2. Experimental transient grating signals of oxidized folded, denatured, and porphyrin cyt *c*.

TABLE 1: Fit Parameters for TG Measurements

	A_1	τ_1 (fs)	A_2	τ_2 (fs)	A_3	τ_3 (fs)
pH 7	−17	20	1.0	140	0.05	1100
pH 2	−23	20	0.77	190	0.18	1200
pH 2/urea	−10	26	0.98	100	0.3	1100
reduced	−8.0	23	0.89	130	0.22	2200
porphyrin	0.68	10^5 [a]	−0.05	280	N/A	N/A

[a] Fixed parameter.

Porphyrin cyt *c* was prepared by removing the iron from the oxidized protein with HF.[33] Protein concentrations were adjusted to give an absorbance of 0.5−0.6 at the excitation wavelength (150−200 μM). Pulse energies of 2−10 nJ per beam were used to perform each TG or 3PEPS experiment. Pulse energies of more than 20 nJ per beam had no effect on the shape of the signals. Pump pulse energies of 5 nJ and probe pulse energies of less than 1 nJ were used for TA measurements.

III. Results

A. Transient Grating Measurements. The TG signals for oxidized cyt *c* are shown in Figure 2, including folded, pH 2.0 unfolded, and urea (pH 2.0) unfolded proteins. Very small amplitude oscillations were observed that were due to impulsively excited vibrations. Parameters for multiexponential fits are collected in Table 1. At the earliest times (<30 fs) the signals from all three samples are dominated by a coherence spike. After the coherence spike, which was fit to a 15 fs exponential, each signal shows a negative amplitude component (rise time) with a time constant of 20−25 fs. For the unfolded proteins, the rising components were apparent from visual inspection of the TG signals. However, for the folded protein, fits that include pulse convolution are required to discern the rise. Due to the short time scale of this rise time the fitted value is strongly correlated with the amplitude and time constant used for modeling the coherent spike. Thus, there is considerable uncertainty in the fit value. However, the data are not well fit by rise times longer than ∼30 fs. The rise in each signal is followed by a biphasic decay with a large amplitude faster component and small amplitude slower component. The fast population dynamics of the excited cyt *c* are reflected in the time scales of the decays: all signals go to zero within a few picoseconds. As discussed below, the initially excited B state is short-lived, so the TG signals at times greater than 100 fs must result from a ground state bleach or an induced absorption from either the ground or Q state. For folded cyt *c*, the two decays occurred with a time constant of 140 fs and 1.1 ps, respectively. The biexponential

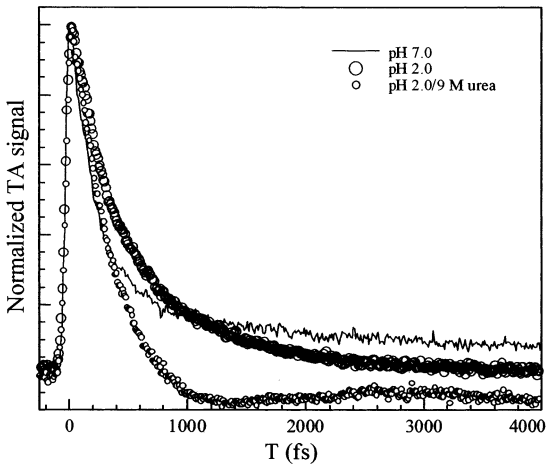

Figure 3. Experimental transient absorption signals of oxidized folded and denatured cyt *c*.

TABLE 2: Fit Parameters for TA Measurements

	A_1	τ_1 (fs)	A_2	τ_2 (fs)	A_{osc}	τ_{damp} (fs)	ω cm^{-1}	ϕ
pH 7	1.09	200	0.2	3700	N/A	N/A	N/A	N/A
pH 2	0.61	250	0.56	790	N/A	N/A	N/A	N/A
pH 2/urea	1.3	360	−0.08	$>10^5$	0.05	3400	23	2.0

decays of the unfolded proteins were fit with a time constant of 190 and 100 fs (pH 2 and urea (pH 2.0), respectively) for the large amplitude component, and a time constant of 1.1 to 1.2 ps (for both unfolded proteins) for the small amplitude component. A TG measurement of porphyrin cyt *c* was also performed (Figure 2). The TG signal showed a coherent spike, with an amplitude similar to those of the other protein samples. The spike is followed by a small amplitude rising component with a time constant of 280 fs, and no decay on a time scale less than 10 ps.

A TG measurement was also performed with the reduced folded protein (Supporting Information). Except for the longest time constant, the TG signal for the reduced protein is similar to that for the oxidized protein. A 23 fs rise, 130 fs decay, and 2.2 ps decay were observed.

B. Transient Absorption Measurements. The TA signals for folded and unfolded cyt *c* are shown in Figure 3. Parameters for multiexponential fits are collected in Table 2. The TA signals for the unfolded proteins show biphasic decays similar to those of the TG signals. The largest discrepancy between the TA and TG results is that the TA signal for urea (pH 2.0) protein becomes negative for times longer than 700 fs, and does not decay on time scales less than 10 ps. As with the TG signals, the TA signals at times greater than 100 fs must result from a ground-state bleach or an induced absorption from either the ground or Q state. In addition, the TA of the urea (pH 2.0) protein shows an oscillatory low frequency component (ω = 23 cm^{-1}). This low frequency vibration has a period longer than that of the B and Q lifetimes (see below) and must therefore correspond to ground state motion. It is unclear why this mode is present only in the urea (pH 2.0) sample. At pH 7.0, the TA signal showed a slow decay (2 ps) that was not present in the TG experiments, whose amplitude was approximately 15% of the total decay.

C. Three-Pulse Photon Echo Peak Shift Measurements. To separate the contribution of homogeneous and inhomogeneous processes to the spectra of both the folded and unfolded proteins, 3PEPS measurements on both folded and denatured cyt *c* were performed (Figure 4). The initial peak shifts for the

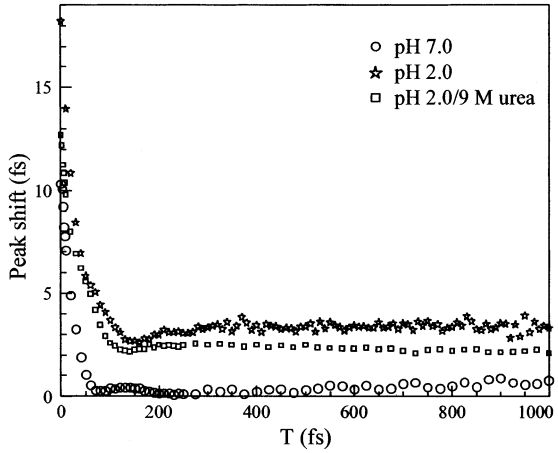

Figure 4. Three pulse echo peak shift data for oxidized folded and unfolded cyt *c*.

proteins are different, with the largest shift observed for the pH 2.0 sample (18 fs), and smallest (10 fs) for the pH 7.0 sample. The intensity of the echo signal rapidly decreases in a few tens of femtoseconds, which made characterization of the folded and pH 2.0 denatured proteins difficult at long population times. The resulting signal-to-noise introduced some uncertainty in the terminal peak shift of the folded protein, but the value did not exceed 1 fs. A small concentration of unfolded protein that is preferentially sampled when the excitation wavelength is tuned to the high energy edge of the spectrum may contribute to the small nonzero asymptotic value. The 3PEPS decay for folded porphyrin cyt *c* was similar to that for folded cyt *c*; however, because of the increased ground state recovery time (see below) the signal was conveniently measured out to a population time of 30 ps. The porphyrin cyt *c* signal showed a 12 fs initial peak shift and a decay to an asymptotic value of 0.5 fs in less than 100 fs. The unfolded proteins show clear and reproducible nonzero asymptotic peak shifts in excess of 2.5 fs. 3PEPS measurements of a control chromophore (1 mM 8-methoxypyrene-1,3,6,trisulfonic acid) at the same wavelength in water reproducibly demonstrated a zero terminal peak shift, indicating that the optical setup does not introduce an artificial nonzero peak shift. Therefore, the pH 2.0 and the urea (pH 2.0) samples asymptotically approach different nonzero peak shifts at long *T*, while the pH 7.0 sample essentially approaches a value of zero.

IV. Multilevel Response Function Formalism

The response function formalism developed by Mukamel and others provides a unified framework that may be used to analyze data from the various time-domain spectroscopies. The data are usually interpreted in the context of a two-level system coupled to a harmonic bath that represents the chromophore and solvent or protein motions.[34] The amplitude and time dependence of these motions cause fluctuations of the electronic energy gap, $\hbar\omega_{eg}$. These fluctuations determine the optical line broadening and the nonlinear optical response. The time dependence of ω_{eg} for each molecule, *i*, may be expressed as

$$\omega^i_{eg}(t) = \langle\omega_{eg}\rangle + \epsilon_i + \delta\omega_{eg}(t) \quad (1)$$

where $\langle\omega_{eg}\rangle$ is the average value of the transition frequency, ϵ_i is a static offset from the average value, and $\delta\omega_{eg}(t)$ describes the dynamics of the fluctuations. The dynamics can be described by the time correlation function of the transition frequency, $M(t)$:

$$M(t) = \frac{\langle \delta\omega_{eg}(0)\delta\omega_{eg}(t)\rangle}{\langle \delta\omega_{eg}^2\rangle} \quad (2)$$

In the high-temperature limit, the complex line broadening function for the optical transition can be written as

$$g(t) = \langle\Delta\rangle^2 \int_0^t dt_1 \int_0^{t_1} dt_2 M(t_2) - i\lambda \int_0^t dt_1 [1 - M(t_1)] + \frac{1}{2}\Delta_{in}^2 t^2 \quad (3)$$

in which Δ is the coupling strength ($\langle\Delta\rangle^2 = (2k_BT\lambda/\hbar)$), Δ_{in} is the inhomogeneous broadening, and λ is the total reorganization energy. This line broadening function is used for calculating the response functions R_{GG} and R_{BB} (rephasing diagrams only), which correspond to time evolution in ground and excited states, respectively,

$$R_{GG}(t,T,\tau) = R^{Re}(t,T,\tau)\exp[iQ_{GG}(t,T,\tau)] \quad (4)$$

$$R_{BB}(t,T,\tau) = R^{Re}(t,T,\tau)\exp[iQ_{BB}(t,T,\tau)] \quad (5)$$

where

$$R^{Re}(t,T,\tau) = \exp[-P(\tau) - P(t) + P(T) - P(\tau+T) - P(T+t) + P(\tau+T+t)]$$

$$Q_{GG}(t,T,\tau) = Q(\tau) - Q(t) - Q(T) + Q(\tau+T) + Q(T+t) - Q(\tau+T+t)$$

$$Q_{BB}(t,T,\tau) = Q(\tau) + Q(t) + Q(T) + Q(\tau+T) - Q(T+t) - Q(\tau+T+t) \quad (6)$$

in which R^{Re} is the modulus of the response function, and P and Q are the real and imaginary parts of $g(t)$, respectively.

In the impulsive limit, the TG and 3PEPS signals associated with the phase-matched direction $-k_1+k_2+k_3$ can be expressed in terms of the response functions

$$S(T,\tau) = \int_0^\infty dt|P^{(3)}(t,T,\tau)|^2 \propto \int_0^\infty dt|R(t,T,\tau)|^2 \quad (7)$$

where $R(t,T,\tau) = \sum_i R_i(t,T,\tau)$ is the sum of contributions from different time-ordered light-matter interactions and time evolutions (for TG experiments $\tau = 0$). The essence of the experiment may be understood by considering the evolution of the system during three time periods that are established by the three pulses. During a first coherence period, initiated by the first pulse, the electronic coherence within the ensemble of absorbing molecules dephases (for time τ). During the population period initiated by the second pulse (for time T) no dephasing is possible, but environmental fluctuations continue. Finally, a second coherence period (of duration t) is initiated by the third pulse. The ensemble may then rephase and emit an echo (at $t = \tau$) if protein and chromophore vibrations have not uncorrelated the two coherence period environments. The response functions used in this manuscript are labeled with two subscripts, $R_{AB,CD}$, to define the state of the system during the population period and second coherence period. For cases where the reactive system visits more than one state during T, those states are set in parentheses. Each response function describes one of eight possible time-orderings of light-matter interactions. However, in the impulsive limit with a fixed time ordering, only two, $R_{GG,BG}$ and $R_{BB,BG}$, are capable of rephasing and generating an echo signal in the simple two-state system. The two corresponding Feynman diagrams, labeled (a) and (b), are shown in Figure 5.

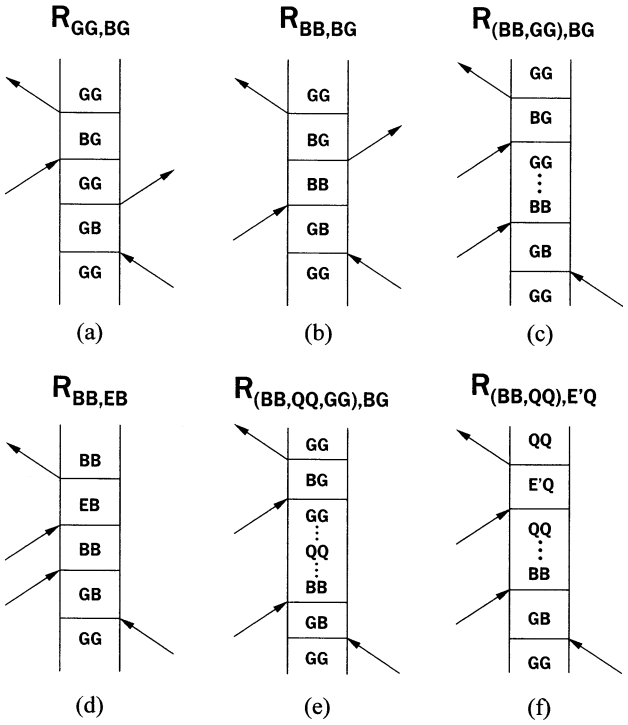

Figure 5. Double-sided Feynman diagrams for cyt *c*.

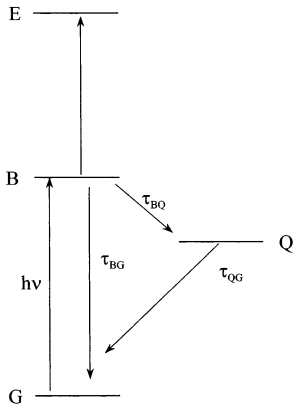

Figure 6. Diagram of cyt *c* electronic states on which the kinetic model is based.

The third-order nonlinear optical response of the three-level cyt *c* system may be described by a modification of the two-state response formalism described above.[30−32] First, any new photophysics (optical transitions, internal conversions, finite lifetimes, chemical reactions, etc.) must be accounted for by the inclusion of additional response functions. Second, all response functions must be modified to account for population changes. If the lifetimes of the states are long compared to the coherence period (τ), as is always the case with TA and TG, the population changes may be incorporated by scaling the response functions with exponential functions corresponding to the time dependent populations (assuming Markovian population kinetics separable from nuclear dynamics).[30]

In Figure 6, a multilevel state diagram is shown for cyt *c* which includes the ground (G), Soret (B), and Q states. The internal conversion processes that may contribute to the photophysics of the heme are also indicated in Figure 6. The description of the nonlinear signal from cyt *c* may include four response functions in addition to those from the two-state

system. The corresponding Feynman diagrams are labeled (c)−(f) in Figure 5. Two response functions are associated with excited state absorption (ESA) from the B and Q states, $R_{BB,EB}$ and $R_{(BB,QQ),E'Q}$, respectively. Two response functions are associated with the ground state recovery: one for the pathway B to Q to G, $R_{(BB,QQ,GG),BG}$; and one for internal conversion directly from B to the ground state, $R_{(BB,GG),BG}$. The total response function is then

$$R = R_{BB,BG} + R_{GG,BG} - R_{BB,EB} - R_{(BB,QQ),E'Q} - R_{(BB,QQ,GG),BG} - R_{(BB,GG),BG} \quad (8)$$

where the negative sign associated with the last four terms is due to the odd number of interactions with the ket and bra sides of the double-sided Feynman diagrams (Figure 5). The contributions of ESA to the signals (i.e., rise or decay) will depend on the correlation between fluctuations of the ground state transition and those for the excited state transition. These contributions are also scaled by the population dynamics, which are rising or decaying functions, depending on whether it is the Q state or the B state that is being monitored. The relative magnitudes of these two factors will determine whether ESA terms contribute a rise or decay in the TG and 3PEPS signals. However, we may dismiss $R_{(BB,QQ),E'Q}$ because the TA spectrum of the folded protein reported by both Champion and co-workers[35] and Jongeward and co-workers[36] show that absorption is significant only at wavelengths significantly to the red of the steady state absorption maximum. Therefore, only ESA from the B state ($R_{BB,EB}$) is considered.

As already mentioned, these response functions need to be scaled according to the population kinetics. Thus, each response function may be separated into a nuclear and a kinetic component (the nuclear component is labeled with a superscript "0"). The B state response functions ($R_{BB,BG}$ and $R_{BB,EB}$) decay as an exponential function of the Soret lifetime, τ_{Soret}. A constant scaling term, μ, is also included to account for the different magnitudes of the EB and GB transition moments.

$$\tau_{Soret} = \left(\frac{1}{\tau_{BG}} + \frac{1}{\tau_{BQ}}\right)^{-1} \quad (9)$$

$$R_{BB,BG} = R^0_{BB,BG} \times \exp[-T/\tau_{Soret}] \quad (10)$$

$$R_{BB,EB} = \mu R^0_{BB,EB} \times \exp[-T/\tau_{Soret}] \quad (11)$$

The first ground state recovery term, $R_{(BB,QQ,GG),BG}$ is scaled as shown in eq 12. This term corresponds to the path from B to Q to G and accounts for population transfer from B to Q while the population is also decaying from B to G. (If $\tau_{BQ} \ll \tau_{BG}$ and $\tau_{BQ} \ll \tau_{QG}$, this term would correspond to an exponential rise on the τ_{QG} time scale.)

$$R_{(BB,QQ,GG),BG} = R^0_{(BB,QQ,GG),BG} \times \left[\frac{\tau_{Soret}}{\tau_{BQ}}(1 - e^{-T/\tau_{Soret}}) + \frac{\tau_{BQ}^{-1} e^{-T/\tau_{QG}}}{\tau_{QG}^{-1} - \tau_{Soret}^{-1}}(1 - e^{T(\tau_{QG}^{-1} - \tau_{Soret}^{-1})})\right] \quad (12)$$

The second ground state recovery term, $R_{(BB,GG),BG}$, is scaled by two terms (equation 13), a prefactor corresponding to the (B to G)/(B to Q) branching ratio and an exponential term describing the population remaining in the B state.

$$R_{(BB,GG),BG} = \left(1 - \frac{\tau_{Soret}}{\tau_{BQ}}\right) R^0_{(BB,GG),BG} \times (1 - \exp[-T/\tau_{Soret}]) \quad (13)$$

If the nuclear history effect is neglected, $R^0_{(BB,QQ,GG),BG} = R^0_{(BB,GG),BG} = R^0_{GG,BG}$, and expressions 12 and 13 may be rearranged to give

$$R_{GG,BG} - R_{(BB,QQ,GG),BG} - R_{(BB,GG),BG} = R^0_{GG,BG} - \frac{\tau_{Soret}}{\tau_{BQ}} R^0_{GG,BG}(1 - e^{-T/\tau_{Soret}}) + R^0_{GG,BG} \frac{\tau_{BQ}^{-1} e^{-T/\tau_{QG}}}{\tau_{QG}^{-1} - \tau_{Soret}^{-1}}(1 - e^{T(\tau_{QG}^{-1} - \tau_{Soret}^{-1})}) \quad (14)$$

Thus, the total response function is then written

$$R = R^0_{BB,BG} \times \exp[-T/\tau_{Soret}] - \mu R^0_{BB,EB} \times \exp[-T/\tau_{Soret}] + R^0_{GG,BG} - \frac{\tau_{Soret}}{\tau_{BQ}} R^0_{GG,BG}(1 - e^{-T/\tau_{Soret}}) + R^0_{GG,BG} \frac{\tau_{BQ} e^{-T/\tau_{QG}}}{\tau_{QG}^{-1} - \tau_{Soret}^{-1}}(1 - e^{T(\tau_{QG}^{-1} - \tau_{Soret}^{-1})}) \quad (15)$$

This multilevel model shows that both ground state and excited state contributions to the signal are influenced by the population dynamics, and that ESA from the Soret excited state makes a negative contribution to the signal. For simplicity, the model does not include a separate time scale for ground state rethermalization. Thus, internal conversion time scales that appear in this expression as a result of ground state recovery (τ_{BG} and τ_{QG}) will appear in the experimental signals as composites of internal conversion and rethermalization. The model also assumes that populations do not change during the coherence periods. In the impulsive limit, this assumption is valid for the discussion of the TG signal, in which $\tau = 0$. However, even in the impulsive limit, this assumption is not expected to be valid for the 3PEPS experiment, as the Soret excited state lifetime (40−50 fs, see below) is comparable to the time scale of the coherence period. Therefore, the model is applicable to all time scales for the TG and TA experiments but only the long time scales ($T > \tau_{Soret}$) for the 3PEPS signals.

V. Discussion

The multilevel photophysics of cyt *c* have been characterized with three ultrafast nonlinear spectroscopic experiments.[34,21] TA and TG measurements are sensitive to population kinetics and solvation dynamics time scales. However, changes in electronic state result in larger changes in the transition moment than does motion along vibrational coordinates. As a result the TG and TA signals for these multilevel systems will predominantly reflect changes in electronic state rather than vibrational dynamics. In contrast, the 3PEPS measurement is sensitive to the time-dependent loss of memory of the electronic transition frequency due to vibrational modes of the chromophore and fluctuations of the environment (protein dynamics). A static distribution of electronic transition energies due to heterogeneity of the chromophore environment (inhomogeneous broadening) is manifested in the 3PEPS measurement as a nonzero asymptotic peak shift, even in the presence of internal conversion processes. To interpret the observed time-domain data, a model response function that incorporates the effects of internal

conversion among multiple electronic states was derived above. The dynamics included in the model are consistent with those reported by Champion and co-workers for the reduced protein.[35] The TA, TG, and 3PEPS results are interpreted in terms of the model response function to derive a consistent picture of the internal conversion time scales and mechanisms of spectral line broadening in the folded and unfolded oxidized proteins.

A. Cytochrome *c* Level Kinetics: Transient Absorption and Transient Grating Measurements. The time scales observed in the TA and TG experiments with each folded state of the oxidized protein, as well as those in the TG experiment with the reduced protein, are qualitatively similar. For all protein forms, three time scale regimes are observed and are assumed to result from analogous processes. Thus, the TA and TG results are discussed without reference to the folded or redox state of the protein.

Each experiment was performed with excitation pulses of 407 nm (folded proteins) and 400 nm (unfolded proteins). As a result, the laser wavelength in each measurement was not tuned to the same spectral position relative to the protein's Soret band "0−0" transition. The wavelength dependence of the signal may be significant, and therefore TG and TA experiments may show different time scales that represent the same dynamics. A 40 to 50 fs rise from the TG data is not present in the TA data, possibly due to a differing amplitude of a coherent artifact in the two signals. The TA and TG measurements each show two longer time scale processes. These time scales are 200 to 400 fs and 2 to 4 ps. The time constants from the two experiments agree qualitatively but not quantitatively. The largest discrepancies between the two experiments are for the smallest amplitude, longest time scale components, which are assigned to ground state recovery. For example, the urea (pH 2) TA data show a negative signal at times longer than 800 fs, which is not observed in the TG signal. This discrepancy may reflect the differing ability of the two techniques to monitor relaxation processes within the ground state.[32] It has been noted before that TA is more sensitive to small amplitude decay components than is TG.[32] Furthermore, TA is only sensitive to the real part of the third order polarization, whereas TG measures both real and imaginary parts of the polarization. Due to this sensitivity of TG to both real and imaginary parts of the polarization, the phases of ground and excited state population gratings will interfere, especially in a multilevel system. Therefore the TA and TG signals may show distinct kinetics. The dynamics in cyt *c* that might give rise to the observed time scales are now discussed.

The TG signals may be calculated in the impulsive limit by inserting eq 15 into eq 7. A direct fit of the data requires convolution of the response functions with the optical pulse and the inclusion of nonrephasing contributions to the signal. However, these calculations may be used to determine the general properties of the TG signal. The values for the response functions $R_{GG,BG}$ and $R_{BB,BG}$ are calculated according to the procedures described in section 4 by assuming a model $M(t)$ function with a 50 fs Gaussian decay ($\lambda = 225$ cm^{-1}) and an inhomogeneous broadening of 100 cm^{-1}. The most difficult issue in modeling the nonlinear response of a three level system is the choice of $M(t)$ for the excited state transition. For the calculations described here, it is assumed that the fluctuations of the transition energy while the molecule resides in either the ground or excited state are the same, thus the same $M(t)$ is used. The effects of relaxing this assumption have been described previously.[31] It is also assumed that $\mathrm{Im}\{R_{BB,EB}\} = 0$, which is reasonable for high temperatures.[22,37] Simulated TG signals for various values of τ_{BG}, τ_{BQ}, τ_{QG}, and μ are shown in Figure 7. A rise time is present for values of μ greater than one, and $\tau_{BQ} < \tau_{BG}$. In these cases, the simulated signals show a fast decay, a rise time associated with τ_{Soret}, and a decay on the time scale of the ground state recovery. The TG signal does not show a decay time scale that is directly associated with τ_{BG}, instead the ratio τ_{BG}/τ_{BQ} determines the amplitude of the τ_{QG} decay component.

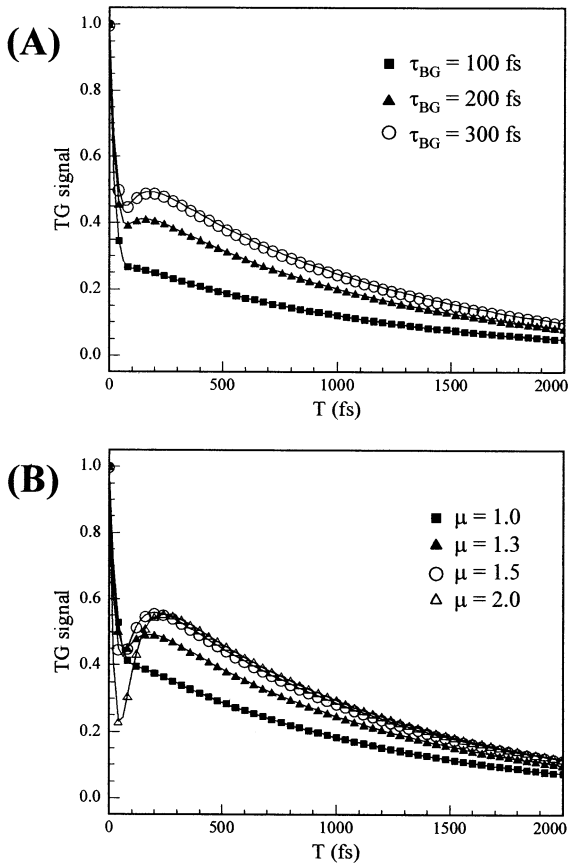

Figure 7. Simulated TG signals, in the impulsive limit, for the three-level system model response function described in the text (eq 15). An $M(t)$ function with a 50 fs Gaussian component ($\lambda = 225$ cm^{-1}) and 100 cm^{-1} inhomogeneous broadening is used to calculate the reaction-free response functions. In (A), internal conversion times cales of $\tau_{BQ} = 80$ fs and $\tau_{QG} = 2200$ fs are assumed, $\mu = 1.4$, and τ_{BG} is varied from 100 to 300 fs. In (B), the value of the transition moment weighting factor, μ, is varied over the range from 1.0 to 2.0.

The simulations show that the rising component of the signal may be associated with the decay of population from the Soret excited state. Therefore, a value of 40 to 50 fs (2 × fitted time constant[32]) may be assigned to the Soret lifetime. A rise time of 280 fs was also observed in the porphyrin cyt *c*, which may be assigned to a longer lived B state, relative to cyt *c*. These lifetimes correspond to lifetime broadening of ∼120 cm^{-1} for the cyt *c* proteins (19 cm^{-1} for the porphyrin cyt *c* protein). This represents ∼8% of the observed line width, indicating that ∼92% of the bandwidth results from vibronic and inhomogeneous contributions. These values of lifetime broadening are smaller than the values obtained from a Raman and absorption line shape study of reduced cyt *c* (370 cm^{-1}).[38]

The simulations also predict that the longest time constant observed in the TA and TG experiments, 2 to 4 ps, may be assigned to ground state recovery from the Q state (τ_{QG}), which includes all rethermalization (IVR, ligand rebinding, etc.). These time scales are similar to those observed in reduced cyt *c* and were assigned as ground state rethermalization.[35] Similar time

scales were also observed for vibrational cooling in myoglobin.[39] Therefore, it seems likely that the longest time scales observed in the oxidized protein also correspond to ground state dynamics. The value of τ_{BG} may not be estimated from the simulations because the appearance of the TG signal depends on the precise form of the electronic transition correlation function, $M(t)$, and also depends critically on the effects of pulse convolution at times within the pulse autocorrelation width. Nevertheless, it is clear that the kinetic model for the response functions, including an ESA contribution from the Soret band, qualitatively accounts for the appearance of the data.

The remaining feature of the TA and TG data requiring explanation is the 200 to 400 fs decay component. The porphyrin cyt *c* TG signals do not contain this time constant. The porphyrin is fluorescent (long Q state lifetime)[40] and will show no ligand dynamics. Therefore the presence of this decay in cyt *c* suggests that the 200 to 400 fs is associated with either the shorter Q state lifetime (relative to porphyrin cyt *c*) or ligand dynamics. Champion and co-workers[35] estimated a Q state lifetime of reduced cyt *c* of ~200 fs, which is similar to the value observed for both the oxidized and reduced protein TG experiments reported in this manuscript. However, it is unlikely that this time constant represents the Q state lifetime. The Q state fluorescence yield is at least a factor of 10 lower in the oxidized relative to the reduced protein, which implies a significant decrease in the Q state lifetime upon oxidation. It is therefore more likely that the difference in Q state fluorescence yield reflects the existence of other internal conversion processes. For example, in myoglobin, charge transfer states with lifetimes similar to those observed here for cyt *c* are thought to have a role in ligand dissociation.[41] These processes are outside of the probe spectral window of the current experiments. Experiments which directly excite the Q state would contribute to defining the nature of this process.

The oxidized and reduced proteins are biophysically distinct. It is therefore interesting to note that the TG data for the oxidized and reduced proteins are qualitatively similar. The only significant difference is a 2-fold increase in the longest time constant ascribed to ground state recovery. As suggested by Champion and co-workers,[35] this slow event may correspond to ligand reassociation. Therefore, the Met80 ligand may rebind faster in the oxidized protein than in the reduced protein. Geminate recombination following photodissociation has been extensively studied with small molecule ligands in other hemoproteins, such as myoglobin, and are discussed in terms of conformational substates of the protein.[42,43] The difference in rebinding time scales of the oxidized and reduced proteins may reflect redox-dependent conformational fluctuations.

B. Multilevel Kinetics and Peak-Shift Measurements. For a simple two-level system with a long-lived excited state, the 3PEPS decay time scales reveal the time-dependent fluctuations of the energy gap between the ground and excited electronic state.[21,44] These fluctuations are caused by coupling of the electronic states with chromophore vibrations and motions of the solvent or protein environment. High-frequency vibrational modes of the chromophore ($\omega > 500$ cm^{-1}) and the convolution of the nonlinear response with the electric field of the laser pulse contribute to a sub-50 fs decay component, which usually dominates the peak shift decay. Lower frequency vibrations and protein motions give rise to smaller amplitude peak shift decays on longer time scales (10^2 to 10^5 fs). A static distribution of electronic transition energies due to heterogeneity of the chromophore environment (inhomogeneous broadening) is manifested in the 3PEPS measurement as a nonzero asymptotic peak shift.

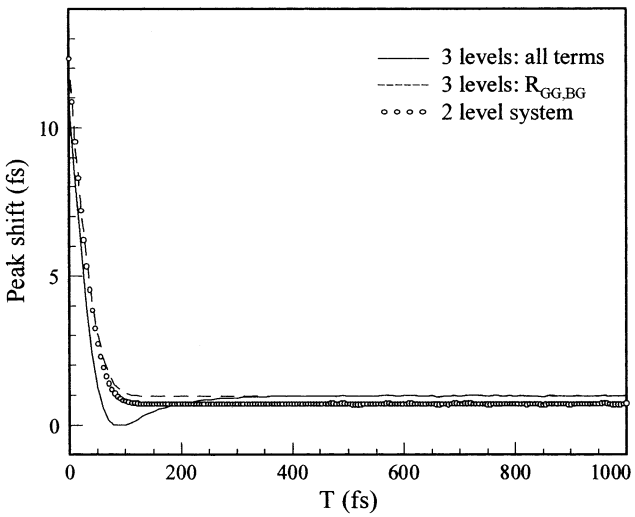

Figure 8. Impulsive limit calculation of 3PEPS decay, using the same $M(t)$ as Figure 7. For the level system, the internal conversion time scales are $\tau_{BQ} = 80$ fs, $\tau_{BG} = 300$ fs, $\tau_{QG} = 2200$ fs, and $\mu = 1.0$. The 3PEPS decays calculated with the $R_{GG,BG}$ term alone, and for the two-level system without internal conversion are also shown. For a three-level system when τ_{BG} is infinite, the 3PEPS decay is identical to the case when only the $R_{GG,BG}$ term is included in the response.

As discussed above, at least three electronic states must be used to describe the photophysics of cyt *c*. The multilevel relaxation dynamics may influence the appearance of the 3PEPS decay as compared to a two-state system. For a two-level system, the value of the initial peak shift, $\tau^*(0)$, is inversely proportional to the inhomogeneous line width.[21] However, when finite bandwidth excitation pulses are used to probe a system with vibronic structure, the value of $\tau^*(0)$ is wavelength dependent.[45,46] Furthermore, for a three-level system with ESA, the $R_{BB,EB}$ term of the response function may contribute to an increase in the value of $\tau^*(0)$, whereas decay to the ground state during the pulse width will contribute to a decrease in the value $\tau^*(0)$.[30] As a result, single wavelength data cannot be used to unambiguously determine the homogeneous line width.

The fastest time scale decay (sub-50 fs) is influenced by a superposition of two effects that decay on the time scale of the Soret excited state lifetime: the decay of the ESA contribution from $R_{BB,EB}$ and the decay of the $R_{BB,BG}$ contribution. After the initial decay, the peak shift either asymptotically approaches a zero value (folded protein), or shows a rise on a ~100 fs time scale followed by asymptotic approach to a nonzero value (both unfolded proteins). In contrast, porphyrin cyt *c* does not show a rise in the peak shift. Since B to G internal conversion is a minor decay route in the porphyrin, the absence of the rise indicates that it is associated with the B to G internal conversion process. There are two different mechanisms by which this internal conversion process may cause a rising peak shift. The first possibility is an interference of the nuclear trajectories between the B-to-G and B-to-Q-to-G pathways. This nuclear history effect was described by Yang et al.[30] However, this effect has been neglected in the model described above. The second possibility arises from the time dependent weighting of the ground state response functions ($R_{GG,BG}$) due to its kinetics. The rise occurs because the magnitude of the ground state contribution to the optical response is decaying. This effect is demonstrated in Figure 8, where impulsive 3PEPS simulations are shown with and without B to G internal conversion using the same model $M(t)$ used for the simulations in Figure 7. A rise is

seen only when τ_{BG} is nonzero and inhomogeneous broadening or other slow dynamics are present. This result demonstrates that the presence of B-to-G internal conversion satisfactorily describes the observed rising peak shift, without the need to invoke the nuclear history effect.

At the longest population delays (*T*), the peak shift shows markedly different behaviors for the 3-folded states of the protein. With the folded cyt *c*, the signal asymptotically approaches zero, as is typically observed for well-ordered systems. With the unfolded proteins, the peak shift asymptotically approaches a value greater than zero. These long time effects must result entirely from ground state contributions ($R_{GG,\ BG}$ and $R_{(BB,\ QQ,\ GG),\ BG}$) since the Q state is dark, and the lifetime of the B state is 40 to 50 fs. Figure 8 demonstrates that when $R_{GG,\ BG}$ is the sole contribution to the echo, which occurs at large *T* due to internal conversion from B to Q, the magnitude of the peak shift is similar to that of the two-level system. Therefore, the long time signal may be interpreted in the same way as the simple two-level system, the decay time scales reflect vibrational dynamics and the asymptotic peak shift reflects inhomogeneous broadening. The value of the asymptotic peak shift in the two unfolded states is also correlated with the Soret band fwhm, indicating that inhomogeneity is a large contribution to spectral broadening in the unfolded proteins. It appears that the folded state of cyt *c* is well ordered, with little inhomogeneity, while the unfolded proteins are more disordered and characterized by larger amounts of inhomogeneity (see below).

C. Unfolding-Induced Changes in Protein and Heme Dynamics. Cytochrome *c* evolved to bind and manipulate the physical properties of the heme cofactor in a manner appropriate for biological functions. It is therefore interesting to consider how the folded state of the protein contributes to the cofactor photophysics. The extremely short (40 to 50 fs) Soret excited state lifetime, which is the result of multiple decay pathways, is not sensitive to protein conformation. However, heme fluorescence does depend on the state of the protein, the Q state becomes slightly fluorescent upon unfolding. Furthermore, we observe that the time constant (2.2 to 2.4 ps) associated with ground state recovery from the Q state does not change significantly upon unfolding, but that its amplitude does change. These observations imply that unfolding of the protein causes the (B-to-G)/(B-to-Q) branching ratio to decrease or that internal conversion processes within the Q state are altered upon unfolding. There are no other significant differences in the TA, TG, or 3PEPS signals for the folded and unfolded protein; time scales of ground state rethermalization, including ligand rebinding, are not dependent upon the native fold of the oxidized protein. The invariance of the rethermalization time scale in the oxidized protein, even during unfolding when the iron ligands are likely to change, is in contrast with the slower rethermalization time scale observed in the TG measurements of the reduced protein. This implies that the reduced protein may be characterized by unusual ligand rebinding dynamics.

These results help deconvolute the varying contributions to the Soret bandwidth in the various forms of the protein. Estimation of the inhomogeneous and lifetime broadening effects demonstrate that >90% of the folded protein Soret bandwidth is due to heme vibrations. Moreover, the very short lifetime of the Soret excited state implies that low-frequency modes are not relaxed before the excited state population decays. This decoupling of low-frequency modes may be related to the lack of temperature-dependent narrowing of the Soret band which has been observed.[47] An increase in inhomogeneous broadening is the dominant contribution to the increased Soret bandwidth in the pH 2.0 sample relative to the pH 7.0 sample. In the urea (pH 2.0) unfolded protein, the Soret band is more narrow than in the folded protein, despite a significant increase in inhomogeneous broadening upon unfolding. Therefore, the homogeneous line width must be much narrower in the pH 2.0 unfolded protein relative to the folded protein. This narrowing must be a vibrational effect (lifetime broadening is similar in the proteins) which likely results from relaxation of out-of-plane distortions imposed on the heme by the native fold.

D. Inhomogeneous Broadening and Conformational Diversity. The protein potential energy surface (PES or energy landscape) has recently received a great deal of attention.[3,48−50] The surface not only determines the protein fluctuations that play critical roles in biological function but also acts to control the folding process. Despite the importance of the PES, it has proven difficult to probe experimentally. A central question regarding the PES is related to its "rugged" or "smooth" character. A rugged surface corresponds to the existence of local minima, with potentially unique heme environments, separated from other minima by barriers that are significant relative to *kT*. A rugged surface will thus be manifested spectroscopically as inhomogeneous broadening. This static distribution of unique heme environments will preserve a rephasing capacity of the electronic coherence, irrespective of the duration of the 3PEPS population period, *T*; even at long *T*, an echo will contribute to the signal. Thus, inhomogeneous broadening is observed as an asymptotic approach of the peak shift to a non zero value. In fact, the magnitude of the nonzero asymptotic value is proportional to the inhomogeneous broadening, and thus to the spectroscopic diversity of heme environments. This proportionality is illustrated in eq 16,[21] which relates the static peak shift ($\tau^*(8)$) to the ratio of the inhomogeneous broadening (Δ_{in}) and total broadening ($\Delta_{in}^2 + \Gamma$):

$$\tau^*(\infty) \approx \frac{1}{\sqrt{\pi}} \frac{\Delta_{in}^2}{(\Delta_{in}^2 + \Gamma)} \tag{16}$$

Since spectroscopic diversity is expected to be proportional to conformational diversity, the nonzero asymptotic peak shift measures the conformational diversity of the protein and the ruggedness of the PES.

The small asymptotic peak shift for the oxidized folded form of cyt *c* indicates that there is little conformational diversity and the state is well-ordered. In contrast, significant asymptotic values of the peak shift for the two unfolded states of the protein indicate the presence of structural heterogeneity. These unfolded forms of the protein must exist in multiple spectroscopically distinct conformations that are separated from each other by barriers significantly in excess of *kT*. It is particularly interesting that the inhomogeneity, and therefore the conformational heterogeneity, of the two unfolded proteins are not the same. Although cyt *c* is known to be a "random coil" under both unfolded conditions,[5] it seems that each state is characterized by differing amounts of polypeptide ordering, at least as sensed by the heme cofactor. Therefore, each form of the protein folds to a well-ordered native state by moving toward the global minimum of the PES from topologically distinct regions of the PES.

VI. Conclusions

Transient absorption, transient grating, and 3PEPS experiments have been used to characterize heme photophysics in cyt *c* and its relationship to the protein. The results were interpreted in terms of a nonlinear optical response function formalism

involving three states: two excited states, and the ground state. The Soret excited-state relaxes by two competing pathways: B-to-G internal conversion and B-to-Q internal conversion. The resulting 40 to 50 fs Soret state lifetime is insensitive to the folded state of the protein. However, the ordered polypeptide environment does affect the partitioning of the relaxation pathways. A 200−400 fs process, which may correspond to population relaxation from the Q state or some other state, results in vibrationally hot ground state which rethermalizes on the ps time scale.

The native fold of the protein provides a well-ordered heme environment that is characterized by little spectroscopic heterogeneity. Loss of the native fold by acid denaturation results in a significant increase in the heterogeneity of the protein. The two unfolded states of the protein are not equally disordered as the addition of urea localizes the ensemble to a smaller set of states, or to a set of states with less spectroscopic diversity. This characterization of structural heterogeneity should be applicable not only to the fully folded or unfolded proteins, but also to folding intermediates. The quantitation of conformational heterogeneity during the folding process would characterize the shape of the PES, which not only controls the folding process but also the structure and fluctuations of the protein that are critical for biological functions. Further studies are currently in progress.

Acknowledgment. This work was funded by the Skaggs Institute for Chemical Biology. We thank Prof. Taiha Joo, Prof. Jake Petrich, Dr. Yutaka Nagasawa, and Dr. Mino Yang for helpful discussions.

Supporting Information Available: Figure showing a TG measurement performed with the reduced folded protein. This material is available free of charge via the Internet at http://pubs.acs.org.

References and Notes

(1) Wilson, M. In *Cytochrome c a multidisciplinary approach*; Scott, R. A., Mauk, A. G., Eds.; University Science Books: Sausalito, CA, 1996.
(2) Bushnell, G. W.; Louie, G. V.; Brayer, G. D. *J. Mol. Biol.* **1990**, *214*, 585−595.
(3) *Special Issue on Protein Folding*; Winkler, J. R., Gray, H. B., Eds.; American Chemical Society: Washington, DC, 1998; Vol. 31, pp 697−773.
(4) Hagihara, Y.; Tan, Y.; Goto, Y. *J. Mol. Biol.* **1994**, *237*, 336−348.
(5) Tsong, T. Y. *Biochemistry* **1975**, *14*, 1542−1547.
(6) Stellwagen, E. *Biochemistry* **1968**, *7*, 2893−2898.
(7) Babul, J.; Stellwagen, E. *Biochemistry* **1972**, *11*, 1195−1200.
(8) Eaton, W. A.; Hochstrasser, R. M. *J. Chem. Phys.* **1967**, *46*, 2533−2539.
(9) Champion, P. M.; Lange, R. *J. Chem. Phys.* **1980**, *73*, 5947−5957.
(10) Champion, P. M.; Perreault, G. J. *J. Chem. Phys.* **1981**, *75*, 490−491.
(11) Shibata, Y.; Takahashi, H.; Kaneko, R.; Kurita, A.; Kushida, T. *Biochemistry* **1999**, *38*, 1802−1810.
(12) Manas, E. S.; Wright, W. W.; Sharp, K. A.; Friedrich, J.; Vanderkooi, J. M. *J. Phys. Chem. B* **2000**, *104*, 6932−6941.
(13) Friedman, J. M.; Rousseau, D. L.; Adar, F. *Proc. Natl. Acad. Sci. U.S.A.* **1977**, *74*, 2607−2611.
(14) Pahapill, J.; Rebane, L. *Chem. Phys. Lett.* **1989**, *158*, 283−288.
(15) Jordan, T.; Eads, J. C.; Spiro, T. G. *Protein Sci.* **1995**, *4*, 716−728.
(16) Joo, T.; Jia, Y.; Yu, J.-Y.; Lang, M. J.; Fleming, G. R. *J. Chem. Phys.* **1996**, *16*, 6089−6108.
(17) Passino, S. A.; Nagasawa, Y.; Joo, T.; Fleming, G. R. *J. Phys. Chem. A* **1997**, *101*, 725−731.
(18) Larsen, D. S.; Ohta, K.; Fleming, G. R. *J. Chem. Phys.* **1999**, *111*, 8970−8979.
(19) Lee, S.-H.; Lee, J.-H.; Joo, T. *J. Chem. Phys.* **1999**, *110*, 10969−10977.
(20) Lang, M. J.; Jordanides, X. J.; Song, X.; Fleming, G. R. *J. Chem. Phys.* **1999**, *110*, 5884−5892.
(21) Cho, M.; Yu, J.-Y.; Joo, T.; Nagasawa, Y.; Passino, S. A.; Fleming, G. R. *J. Phys. Chem.* **1996**, *100*, 11944−11953.
(22) Nagasawa, Y.; Passino, S. A.; Joo, T.; Fleming, G. R. *J. Chem. Phys.* **1997**, *106*, 4840−4852.
(23) Nagasawa, Y.; Yu, J.-Y.; Fleming, G. R. *J. Chem. Phys.* **1998**, *109*, 6175−6183.
(24) Jordanides, X. J.; Lang, M. J.; Song, X.; Fleming, G. R. *J. Phys. Chem. B* **1999**, *103*, 7995−8005.
(25) Groot, M.-L.; Yu, J.-Y.; Agarwal, R.; Norris, J. R.; Fleming, G. R. *J. Phys. Chem. B* **1998**, *102*, 5923−5931.
(26) Yu, J.-Y.; Nagasawa, Y.; van Grondelle, R.; Fleming, G. R. *Chem. Phys. Lett.* **1997**, *280*, 404−410.
(27) Jimenez, R.; van Mourik, F.; Yu, J. Y.; Fleming, G. R. *J. Phys. Chem. B* **1997**, *101*, 7350−7359.
(28) Agarwal, R.; Kruegger, B. P.; Scholes, G. D.; Yang, M.; Yom, J.; Mets, L.; Fleming, G. R. *J. Phys. Chem. B* **2000**, *104*, 2908−2918.
(29) Jimenez, R.; Case, D. A.; Romesberg, F. E. *J. Phys. Chem. B* **2002**, *106*, 1090−1103.
(30) Yang, M.; Ohta, K.; Fleming, G. R. *J. Chem. Phys.* **1999**, *110*, 10243−10252.
(31) Xu, Q.-H.; Scholes, G. D.; Yang, M.; Fleming, G. R. *J. Phys. Chem. A* **1999**, *103*, 10348−10358.
(32) Xu, Q.-H.; Fleming, G. R. *J. Phys. Chem. A* **2001**, *105*, 10187−10195.
(33) Vanderkooi, J. M.; Erecinska, M. *Eur. J. Biochem.* **1975**, *60*, 199−207.
(34) Mukamel, S. *Principles of Nonlinear Optical Spectroscopy*; Oxford: New York, 1995.
(35) Wang, W.; Ye, X.; Demidov, A. A.; Rosca, F.; Sjodin, T.; Cao, W.; Sheeran, M.; Champion, P. M. *J. Phys. Chem. B* **2000**, *104*, 10789−10801.
(36) Jongeward, K. A.; Magde, D.; Taube, D. J.; Traylor, T. G. *J. Biol. Chem.* **1988**, *263*, 6027−6030.
(37) Nagasawa, Y.; Yu, J. Y.; Cho, M. H.; Fleming, G. R. *Faraday Discuss.* **1997**, *108*, 23−34.
(38) Schomacker, K. T.; Champion, P. M. *J. Chem. Phys.* **1986**, *84*, 5314−5325.
(39) Kholodenko, Y.; Volk, M.; Gooding, E.; Hochstrasser, R. M. *Chem. Phys.* **2000**, *259*, 71−87.
(40) Vanderkooi, J. M.; Adar, F.; Erecinska, M. *Eur. J. Biochem.* **1976**, *64*, 381−387.
(41) Franzen, S.; Kiger, L.; Poyart, C.; Martin, J.-L. *Biophys. J.* **2001**, *80*, 2372−2385.
(42) Frauenfelder, H.; Chu, K.; Nienhaus, G. U.; Young, R. D. Barrier crossing phenomena in the heme pocket of myoglobin. In *Activated Barrier Crossing*; Fleming, G. R., Hänggi, P., Eds.; World Scientific: Singapore, 1993.
(43) Srajer, V.; Reinisch, L.; Champion, P. M. *J. Am. Chem. Soc.* **1988**, *110*, 6656−6670.
(44) Fleming, G. R.; Cho, M. *Annu. Rev. Phys. Chem.* **1996**, *47*, 109−134.
(45) Larsen, D. S.; Ohta, K.; Xu, Q.-H.; Cyrier, M.; Fleming, G. R. *J. Chem. Phys.* **2001**, *114*, 8008−8019.
(46) Ohta, K.; Larsen, D. S.; Yang, M.; Fleming, G. R. *J. Chem. Phys.* **2001**, *114*, 8020−8039.
(47) Schomacker, K. T.; Bangcharoenpaurpong, O.; Champion, P. M. *J. Chem. Phys.* **1984**, *80*, 4701−4717.
(48) Radford, S. E. *Trends Biochem. Sci.* **2000**, *25*, 611−618.
(49) Dinner, A. R.; Sali, A.; Smith, L. J.; Dobson, C. M.; Karplus, M. *Trends Biochem. Sci.* **2000**, *25*, 331−339.
(50) Onuchic, J. N.; LutheySchulten, Z.; Wolynes, P. G. *Annu. Rev. Phys. Chem.* **1997**, *48*, 545−600.